Circular RNA EFR3A promotes nasopharyngeal carcinoma progression through modulating the miR-654-3p/EFR3A axis

Pan Jiang, Binghua Xia*

Department of Otorhinolaryngology, Suzhou Ninth People's Hospital, Suzhou, Jiangsu, 215200, China

ARTICLE INFO

ABSTRACT

Nasopharyngeal carcinoma (NPC) originates from the nasopharyngeal epithelium. hsa_circ_0135761 (circEFR3A), a newly identified circRNA, presented elevation in NPC via high-throughput sequencing. This study aimed to clarify the molecular mechanism of circEFR3A in the carcinogenesis of NPC. Based on RT-qPCR, subcellular fractionation, RNase R digestion and actinomycin D assays, we evaluated circEFR3A expression characteristics in NPC cells. We found that the circEFR3A was located in the cytoplasm of NPC cells, presented upregulation and stably expressed in NPC cells. Loss-of-function assays clarified the effects of circEFR3A on NPC cell malignant behaviors. The results demonstrated that circEFR3A knockdown facilitated NPC cell apoptosis but repressed NPC cell proliferation and migration. Furthermore, the regulatory mechanism of circEFR3A in NPC was explored. Bioinformatics and mechanism experiments revealed that cicrEFR3A positively modulated EFR3A by competitively binding with miR-654-3p in NPC cells. Additionally, rescue assays showed that the suppressive effects of cicrEFR3A knockdown on NPC cell proliferation, migration and apoptosis were countervailed by EFR3A upregulation. Xenograft tumor-bearing mouse models were established to investigate the role of cicrEFR3A in NPC tumorigenesis in vivo, and the results indicated that circEFR3A silencing suppressed tumor growth in mice. In conclusion, circEFR3A is highly expressed and functions as an oncogene in NPC progression. circEFR3A facilitates NPC cell proliferation and migration by binding to miR-654-3p to upregulate EFR3A, providing a potential new direction for seeking therapeutic plans for NPC.

Introduction

Nasopharyngeal carcinoma (NPC) originates from the nasopharyngeal epithelium and is particularly prevalent in Southeast Asia, North Africa, the Middle East, and Alaska (1). From the perspective of epidemiology, NPC occurrence may have a relation to genetics, environment or Epstein-Barr virus infection. (2). Approximately 70% of NPC patients develop cervical lymph node metastases, and almost all advanced patients have invasive growths at the base of the skull (3). Nevertheless, so far, molecular mechanisms underlying NPC development, especially metastasis, remain elusive. Thus, it is urgent to seek novel molecular targets.

Circular RNAs (circRNAs) are a special type of long-chain non-coding RNA, containing at least hundreds of nucleotides, a closed-loop structure majorly formed by exon and intron sequences, without 5' cap and 3' tail, thus it is not sensitive to ribonuclease and its expression is relatively stable (4). Most of the mature circRNAs currently researched are derived from exons and are produced by special alternative splicing. There are two types of circRNAs formed by circularization of exons: One is "lasso-driven circularization" formed by covalent binding of exons; the other is "intron pairing-driven circularization" formed by complementary pairing of introns, and then splicing the remaining introns through spliceosome to form various circRNAs (5). CircRNAs have close relation to the stage, tumor size, differentiation and metastasis of cancers (6). Though multiple circRNAs have been identified, the roles of multiple circRNAs remain unclear, especially in NPC. According to the hint of literature, hsa_circ_0135761 (circEFR3A) was identified as a circRNA that presented a marked elevation in NPC via high-throughput sequencing (7). Nevertheless, its molecular mechanism in NPC is still elusive. Recently, some circRNAs have been demonstrated to regulate messenger RNA (mRNA) expression through functioning as a microRNA (miRNA) sponge (8-10). For instance, circRNA_0025202 affects tumor progression via the miR-182-5p/FOXO3a axis in breast cancer (11). Circular RNA CRIM1 acts as a ceRNA to promote NPC metastasis through upregulating FOXQ1 (12). We hypothesized that circEFR3A may exert its role in NPC in such a regulatory pattern.

MicroRNAs (miRNAs) are a cluster of noncoding RNAs that are post-transcriptional negative regulators of mRNA that act by binding to their 3'-untranslated region (3'-UTR), leading to mRNA degradation or translational suppression (13). Abnormal miRNA expression has been implicated in the progression of multiple cancers, NPC included (14). Thus, this research majorly attempted to clarify the molecular mechanism of circEFR3A carcinogenesis underlying NPC, which might provide a potential novel insight for seeking therapeutic plans of NPC.

---

* Corresponding author. Email: xiazige202208@163.com

Materials and Methods

Animals, reagents and antibodies

Human NPC cell lines (C666-1, SUNE1, 5-8F and 6-10B) and immortalized normal nasopharyngeal epithelial cell line (NP69) from Cell Bank, Chinese Academy of Sciences (Shanghai, China); four-week-old male BALB/c nude mice from Animal Resources Laboratory, Chinese Academy of Sciences (Beijing, China); lentivirus carrying shRNA sequence targeting circEFR3A or empty vector (HanBio, Shanghai, China); Lipofectamine 2000 from Invitrogen (USA); short hairpin RNA (shRNA) targeting circEFR3A (sh-circEFR3A-1/2) or shRNA negative control (sh-NC), miR-654-3p mimics, miR-654-3p inhibitor and corresponding negative control, EFR3A overexpression vector (pcDNA3.1-EFR3A) or empty vector (pcDN3.1) from GenePharma (Shanghai, China); primary antibodies including anti-Ki67 (0.1 μg/ml), anti-EFR3A (1/1000) and anti-GAPDH (1/1000) and anti-rabbit horseradish peroxidase-labeled secondary antibody (1/2000) from Abcam (Shanghai, China).

Cell lines and cell culture

C666-1, SUNE1, 5-8F and 6-10B cells and control cell line NP69 were cultured in RPMI-1640 medium containing 10% FBS, 100 U/ml penicillin and 100 U/ml streptomycin at 37°C with 5% CO_2, and cells at logarithmic growth phase were taken for following assays.

RNA extraction and RT-qPCR

The total RNA was extracted from cells using TRIzol reagent (Invitrogen, USA). cDNA was synthesized via random primers and SuperScriptIII reverse transcriptase (Thermo Fisher, USA). RT-qPCR for miR-654-3p was conducted using Bulge-Loop miRNA qRT-PCR Starter Kit (Ribobio, Guangzhou, China) with U6 as internal normalization. For circEFR3A and EFR3A, reverse transcription reactions were performed with Prime Script RT Reagent Kit with GAPDH as internal control. The PCR reaction was run in triplicate with 7500 Real-Time PCR System using SYBR Premix Ex Taq II (TaKaRa). Gene expression was calculated using the $2^{-\Delta\Delta Ct}$ method.

Subcellular fractionation

Cytoplasmic and nuclear RNA was extracted with a Cytoplasmic and Nuclear RNA Purification Kit (Life Technologies, USA). Briefly, C666-1 and SUNE1 cells were collected and incubated for 10 min with lysis solution on ice, and then centrifuged for 3 min at 12000 g. The supernatant was collected for cytoplasmic RNA and nuclear pellet was used for nuclear RNA extraction. GAPDH was used as cytoplasmic endogenous control. U6 was used as nuclear endogenous control.

RNase R and actinomycin D treatment

For RNase R treatment, total RNA (2 μg) was incubated with or without 3 U/μg of RNase R (Epicentre Technologies, Madison, WI, USA) for 1 h at 37°C. For blocking transcription, 2 mg/ml actinomycin D or negative control DMSO (Sigma-Aldrich, MO, USA) was added into the cell culture medium. After treatment with actinomycin D and RNase R, RT-qPCR determined expression levels of circEFR3A and EFR3A mRNA in C666-1 and SUNE1 cells.

Cell transfection

C666-1 and SUNE1 cells were cultured to approximately 80% confluence in plates and then transfected with designated plasmids using Lipofectamine 2000 according to the manufacturer's instructions. After 48 h of transfection, cells were harvested for the next assays.

Colony formation

C666-1 and SUNE1 cells (1×10^3 cells/well) were seeded in a 6-well plate and incubated for 1 week at 37°C. Then, cells were washed twice in PBS, fixed with 4% formaldehyde for 15 min and stained with crystal violet for 30 min. The colonies (a diameter ≥ 100 μm) were counted in triplicate assays.

CCK-8

Cell viability was assessed with a CCK-8 kit (Dojindo Laboratories, Kumamoto, Japan). Briefly, 1×10^3 C666-1 and SUNE1 cells were seeded into each well of 96-well plates for culture plus CCK-8 (10 μL) at 0, 24, 48 and 72 h. Two hours post-incubation, optical density was measured with a microplate reader at 450 nm.

Transwell migration

C666-1 and SUNE1 cells were seeded in each Transwell chamber (Costar Corporation, USA) containing 200 μL of serum-free RPMI-1640 (5×10^5 cells/well). The lower compartment was filled with RPMI-1640 containing 10% FBS. The cells were cultured for 24 h, and cells remaining on the upper surface of the filter membrane were removed, and cells on the below surface of the filter membrane were fixed with methanol, stained with crystal violet, and photographed under a microscope.

Wound healing

C666-1 and SUNE1 cells were positioned in a 6-well plate, and cultured until confluence reached 90%. The monolayer cells were scraped with a 200 μL pipette tip to make a wound. Then cells were cultured with a serum-free medium. After 24 h, wound closure percentage was calculated under a microscope.

Flow cytometry

The apoptosis was detected by combined Annexin V-FITC/PI double staining (BD, Biosciences, USA) method. C666-1 and SUNE1 cells were seeded into cell plates at a density of 5×10^4 cells/well for culture, and then collected 48 h post-transfection. After washing with PBS 3 times, 5 μl of Annexin V-FITC and 10 μl of PI were added, respectively, mixed well and reacted for 10 min at room temperature in the dark. The apoptosis was measured on a flow cytometer.

Western blotting

The logarithmic phase C666-1 and SUNE1 cells were taken, medium in the culture dish was aspirated and cells were stored in a sterile centrifuge tube. After centrifugation at 1200 r/min for 10 min, the lysate was added to resuspend cells. The protein concentration was determined by the BCA method. The 5×SDS gel electrophoresis buffer was added and denatured at 100°C for 10 min. After being completely separated by electrophoresis, the protein was transferred to the PVDF membrane by semi-dry method. After blocked by 5% skimmed milk powder

at room temperature for 2 h, the specific primary antibodies were added, and incubated overnight at 4°C. Then the secondary antibodies were added, incubated for another 2 h, and washed with TBS. Absorbance analysis was performed after color development to calculate the relative expression of each protein.

Luciferase gene reporter

circEFR3A-WT and EFR3A 3'UTR-WT was constructed through miR-654-3p binding site on circEFR3A/EFR3A 3'UTR with pmirGLO vectors. Mutant (MUT) circEFR3A/EFR3A 3'UTR sequence was subcloned to an empty vector for circEFR3A-MUT and EFR3A 3'UTR-MUT. The indicated plasmids received co-transfection with miR-654-3p mimics or mimics NC in C666-1 and SUNE1 cells. Finally, a Dual-Luciferase Reporter Assay System assessed luciferase intensity.

Tumor xenografts

The animal care and use ethics committee of our hospital approved the animal experiments. Four-week-old male BALB/c nude mice were procured by Suzhou Ninth People's Hospital. Subcutaneous injection of C666-1 cells (1×10^6) with sh-circEFR3A-1 or sh-NC into the mouse right side was conducted for tumor growth, named the sh-NC group (n=3) and sh-circEFR3A-1 group (n=3). Tumor volume = length × width^2 × 0.5. Mice were sacrificed 4 weeks post-injection. Tumors were photographed and weighed and then stored at -80°C for subsequent use.

RIP

A Magna RIP RNA-Binding Protein Immunoprecipitation Kit (Millipore, USA) was adopted to determine the relationship between circEFR3A and EFR3A. Antibodies used for the RIP assay were anti-AGO2 and control IgG (Millipore, USA), and the coprecipitated RNAs were evaluated by RT-qPCR.

RNA pull-down assay

NPC cells (1×10^7) were collected and lysed. The biotinylated miR-654-3p probe synthesized by Genepharm (Shanghai, China) was incubated with streptavidin agarose beads (Thermo Scientific). The cell lysate was incubated with miR-654-3p probe overnight at 4°C. RNA complex bound to the beads was eluted, and RT-qPCR was used to measure circEFR3A and EFR3A 3'UTR enrichment pulled down by miR-654-3p probe.

Immunochemistry

Dewaxed and rehydrated tumor slides received treatment of 3% hydrogen peroxide and 5% BSA. The slides received incubation with primary antibody anti-Ki67 (Abcam, USA) overnight, and received subsequent incubation with a secondary antibody for 30 min at room temperature. Sections were counterstained with hematoxylin and observed under a microscope.

Statistical analysis

SPSS 20.0 software processed data. All independent experiments were performed three times. The data were expressed as mean ± standard deviation (m ± s). The mean of samples between groups was compared using t-test, and that of multiple groups through one-way analysis of variance followed by Tukey's post hoc test. The difference was statistically significant upon $P < 0.05$.

Results

Expression characteristics of circEFR3A in NPC cells

Previously, circEFR3A was identified to present a marked elevation in NPC via high-throughput sequencing (7). We wondered why its specific role underlying NPC remains elusive. First, RT-qPCR measured circEFR3A expression status in human NPC cell lines (C666-1, SUNE1, 5-8F and 6-10B) and immortalized normal nasopharyngeal epithelial cell line (NP69). As a result, circEFR3A presented a remarkable upregulation in NPC cells relative to controls (Figure 1A). Additionally, circEFR3A presented the highest level in C666-1 and SUNE1 cells, thus these two cell lines were chosen for the following assays. We then assessed the localization of circEFR3A in NPC cells. Through subcellular fractionation, circEFR3A exhibited predominately cytoplasmic distribution in C666-1 and SUNE1 cells (Figure 1B). As we know, circRNAs are resistant to RNase R stimulation, thus we conducted an RNase R digestion assay in NPC cells. Linear RNA transcript (EFR3A mRNA) showed a marked degradation relative to circEFR3A, further confirming the circular nature of circEFR3A transcript (Figure 1C). Moreover, the stability of two transcripts was evaluated under administration with transcription inhibitor, actinomycin D. RT-qPCR depicted that the half-life of EFR3A mRNA was 6-12 h while that of circEFR3A exceeded 24 h in C666-1 and SUNE1 cells (Figure 1D), demonstrating that circEFR3A transcript presented more stability than linear transcript. Collectively, circEFR3A presents upregulation and stable characteristics in NPC cells.

circEFR3A facilitates NPC cell proliferation and migration

Due to circEFR3A upregulation in NPC cells, we hypothesized that circEFR3A may function as an oncogene in NPC cellular behaviors. Thus, we conducted a series of loss-of-function assays. First, shRNA vectors (sh-circEFR3A-1/2) and control sh-NC were transfected into C666-1 and SUNE1 cells. circEFRE3A level presented a successful silencing after shRNA transfection (Figure 2A). Then, colony formation and CCK-8 assessed NPC cell proliferative capability. As a result, circEFR3A knockdown
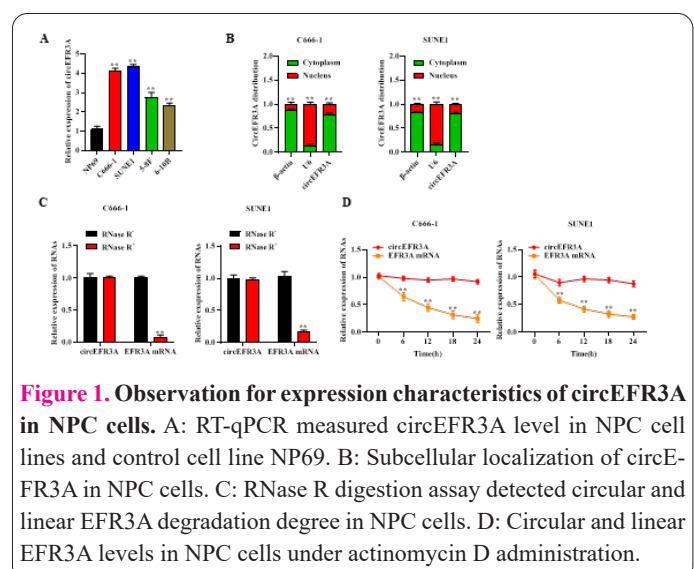

Figure 1. **Observation for expression characteristics of circEFR3A in NPC cells.** A: RT-qPCR measured circEFR3A level in NPC cell lines and control cell line NP69. B: Subcellular localization of circEFR3A in NPC cells. C: RNase R digestion assay detected circular and linear EFR3A degradation degree in NPC cells. D: Circular and linear EFR3A levels in NPC cells under actinomycin D administration.
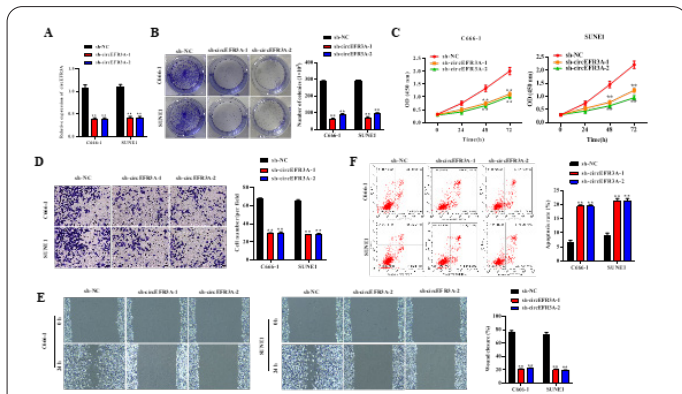
Figure 2. circEFR3A facilitated NPC cell proliferation and migration. A: RT-qPCR detected knockdown efficacy of sh-NC or sh-circEFR3A-1/2 in NPC cells. B: Colony formation assessed NPC cell proliferation under transfection with sh-NC or sh-circEFR3A-1/2. C: CCK-8 assessed NPC cell viability under indicated transfection. D-E: Transwell and wound healing evaluated NPC cell migration under indicated transfection. F: Flow cytometry measured NPC cell apoptosis under indicated transfection.

led to a remarkable reduction of colony amount as well as viability decline in C666-1 and SUNE1 cells (Figure 2B, 2C), suggesting that circEFR3A knockdown suppressed NPC cell proliferation. Moreover, the transwell migration assay demonstrated the decreased migratory cells under circEFR3A silencing (Figure 2D), and the wound healing assay presented a similar trend in migratory cell numbers under circEFR3A knockdown (Figure 2E). Furthermore, flow cytometry illustrated that circEFR3A deficiency facilitated elevation in apoptotic cell proportion in C666-1 and SUNE1 cells (Figure 2F). Collectively, circEFR3A facilitates NPC cell malignant behaviors.

circEFR3A positively regulates EFR3A expression through the ceRNA pattern

We attempted to clarify the association of EFR3A circular and linear transcripts. RT-qPCR depicted that EFR3A level showed depletion under sh-circERF3A-1/2 transfection in NPC cells (Figure 3A). Consistently, western blotting presented a decrease in EFR3A protein abundance under circEFR3A knockdown (Figure 3B). The above results demonstrated that circEFR3A exerted a positive regulation on EFR3A expression. Additionally, UALCAN (http://ualcan.path.uab.edu/) revealed that EFR3A presents elevation in HNSC tissues (Figure 3C). RT-qPCR demonstrated that EFR3A mRNA presented upregulation in NPC cells relative to controls (Figure 3D). As circEFR3A showed cytoplasmic distribution in NPC cells, suggesting that circEFR3A may exert post-transcriptional regulation on gene expression. Thus, we suspected that circEFR3A might positively modulate EFR3A in such a manner. circRNAs have been revealed to play a vital role in various tumors through competing endogenous RNA (ceRNA) networks (15, 16). RIP assay illustrated that both circEFR3A and EFR3A showed a marked enrichment in the anti-Ago group rather than the anti-IgG group (Figure 3E), supporting that circEFR3A may exert regulation on EFR3A through ceRNA pattern. Collectively, circEFR3A may positively modulate EFR3A via the ceRNA network in NPC cells.

circEFR3A upregulates EFR3A through sponging miR-654-3p

CeRNAs are transcripts regulating each other post-transcriptionally through competing for shared miRNAs (17). To further validate the ceRNA pattern of circEFR3A and EFR3A, their common miRNA was screened. Through overlapping results from circBank (http://www.circbank.cn/) and starBase (https://starbase.sysu.edu.cn/index.php), miR-654-3p was identified as a putative common miRNA of circEFR3A and EFR3A (Figure 4A). UALCAN revealed that miR-654-3p presents depletion in HNSC tissues (Figure 4B). RT-qPCR demonstrated that miR-654-3p presented downregulation in NPC cells rela-
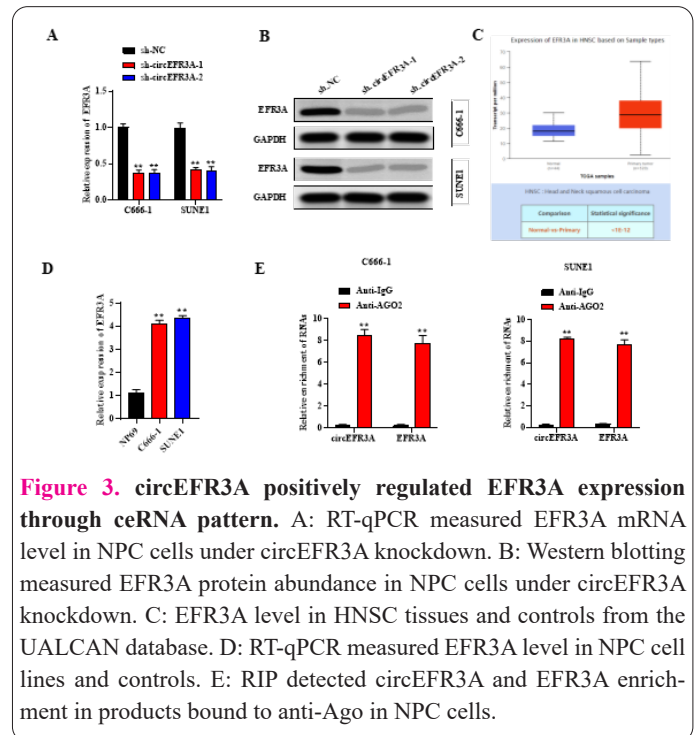

Figure 3. circEFR3A positively regulated EFR3A expression through ceRNA pattern. A: RT-qPCR measured EFR3A mRNA level in NPC cells under circEFR3A knockdown. B: Western blotting measured EFR3A protein abundance in NPC cells under circEFR3A knockdown. C: EFR3A level in HNSC tissues and controls from the UALCAN database. D: RT-qPCR measured EFR3A level in NPC cell lines and controls. E: RIP detected circEFR3A and EFR3A enrichment in products bound to anti-Ago in NPC cells.
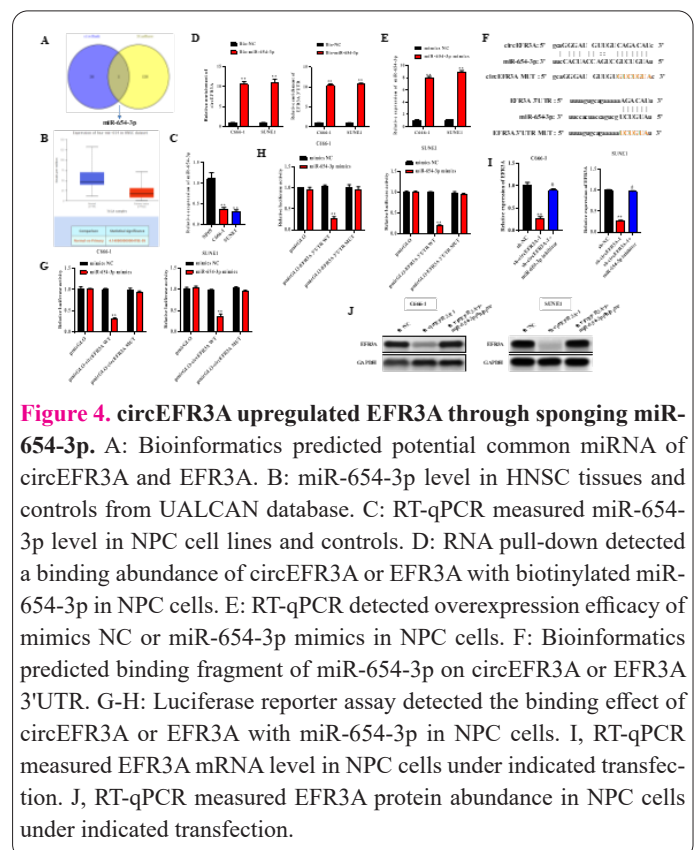

Figure 4. circEFR3A upregulated EFR3A through sponging miR-654-3p. A: Bioinformatics predicted potential common miRNA of circEFR3A and EFR3A. B: miR-654-3p level in HNSC tissues and controls from UALCAN database. C: RT-qPCR measured miR-654-3p level in NPC cell lines and controls. D: RNA pull-down detected a binding abundance of circEFR3A or EFR3A with biotinylated miR-654-3p in NPC cells. E: RT-qPCR detected overexpression efficacy of mimics NC or miR-654-3p mimics in NPC cells. F: Bioinformatics predicted binding fragment of miR-654-3p on circEFR3A or EFR3A 3'UTR. G-H: Luciferase reporter assay detected the binding effect of circEFR3A or EFR3A with miR-654-3p in NPC cells. I, RT-qPCR measured EFR3A mRNA level in NPC cells under indicated transfection. J, RT-qPCR measured EFR3A protein abundance in NPC cells under indicated transfection.

tive to controls (Figure 4C). RNA pull-down demonstrated that both circEFR3A and EFR3A showed abundant enrichment in pull-down products by biotinylated miR-654-3p in C666-1 and SUNE1 cells (Figure 4D). Additionally, miR-654-3p was successfully elevated under transfection with miR-654-3p mimics (Figure 4E). Moreover, wild-type binding sequence of miR-654-3p on circEFR3A or EFR3A 3'UTR was respectively exhibited. Simultaneously, these sequences were mutated (Figure 4F). After mutation, we carried out a luciferase reporter assay to assess their relationships in NPC cells. As a result, the luciferase activity of circEFR3A-WT presented a reduction and that of EFR3A 3'UTR-WT exhibited a similar trend in C666-1 and SUNE1 cells under miR-654-3p upregulation, while both of them showed no marked changes in mutant groups (Figure 4G, 4H). Subsequently, we further clarified the expression association of the circ-EFR3A-miR-654-3p-EFR3A network. EFR3A mRNA and protein levels showed downregulation under sh-circEFR3A-1 transfection and rescued through sh-circEFR3A-1 and miR-654-3p inhibitor cotransfection in NPC cells (Figure 4I, 4J). Collectively, circEFR3A competitively binds to miR-654-3p to upregulate EFR3A.

circEFR3A facilitates NPC cell malignancy via EFR3A elevation

To clarify the ceRNA pattern of circ-EFR3A-miR-654-3p-EFR3A in NPC cellular processes, we conducted rescue experiments. EFR3A level was overexpressed after transfection with pcDNA3.1-EFR3A (Figure 5A). We discovered that the decreased proliferation (Figure 5B), viability (Figure 5C) and migration (Figure 5D, 5E) and elevated apoptosis (Figure 5F) due to circEFR3A silencing were all reversed through EFR3A elevation. Collectively, circEFR3A facilitates NPC cell malignant phenotype via EFR3A upregulation.

circEFR3A contributes to NPC malignant progression in vivo

To clarify circEFR3A role in NPC progression, in vivo xenograft tumor experiments were conducted. After C666-
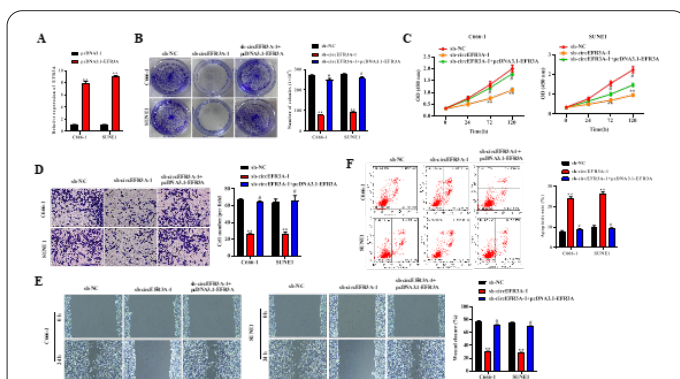

Figure 6. circEFR3A contributed to NPC malignant progression in vivo. A: Pictures of tumors collected from mice under injection with C666-1 cells expressing sh-circEFR3A-1 or sh-NC. B: Tumor volume changes in each group. C: Tumor weight changes in each group. D: Ki67 expression changes in each group.

1 cells expressing sh-circEFR3A were inoculated in mice, the size, volume and weight of tumors were repressed (Figure 6A-C). Furthermore, the expression proportion of Ki67, the marker of proliferation, presented downregulation in tumor tissue (Figure 6D). Collectively, circEFR3A facilitates NPC development in vivo.

Discussion

Increasing evidences has unveiled that the abnormal expressions of circRNAs are associated with the progression of NPC. circRNF13 reduces the proliferation and metastasis of NPC via SUMO2 (18). circTRAF3 facilitates NPC metastasis through miR-203a-3p/AKT3 axis (19). circEFR3A, a newly identified circRNA, has not clarified its role in NPC. Herein, circEFR3A showed upregulation in NPC cells relative to controls, which is consistent with a previous report (7). Its high expression indicates a potential oncogenic role underlying NPC. Moreover, circEFR3A showed a certain stability as a circular transcript. Additionally, circEFR3A silencing suppressed NPC cell proliferation and migration and facilitated NPC cell apoptosis. circEFR3A knockdown reduced xenograft tumor growth in mice. Thus, circEFR3A functioned as an oncogene in NPC via facilitating NPC cell malignancy in vitro and tumor growth in vivo.

circRNAs can bind to miRNAs or RNA-binding proteins (RBPs) post-transcriptionally or during transcription to modulate gene expression (4, 20, 21), and thereby get involved in the progression of multiple diseases. circEFR3A has also been validated its cytoplasmic localization in NPC cells, suggesting its potential post-transcriptional regulation on gene expression. Previously, EFR3A were newly reported in colorectal adenomas (22). Moreover, EFR3A, an adapter protein for the phosphatidylinositol kinase PI4KA, is preferentially bound with oncogenic KRAS (23). As well known, circRNAs can affect cancer progression via regulating their host genes. For example, circITGA7 hinders colorectal cancer growth and metastasis via upregulating transcription of its host gene ITGA7 (24). circGOT1 enhances cell proliferation and mobility in esophageal squamous cell cancer via regulating its host

Figure 5. circEFR3A facilitated NPC cell malignancy via EFR3A elevation. A: RT-qPCR detected overexpression efficacy of pcDNA3.1 or pcDNA3.1-EFR3A in NPC cells. B: Colony formation assessed NPC cell proliferation under transfection with sh-NC, sh-circEFR3A-1 or sh-circEFR3A+pcDNA3.1-EFR3A. C: CCK-8 assessed NPC cell viability under indicated transfection. D-E: Transwell and wound healing evaluated NPC cell migration under indicated transfection. F: Flow cytometry measured NPC cell apoptosis under indicated transfection.
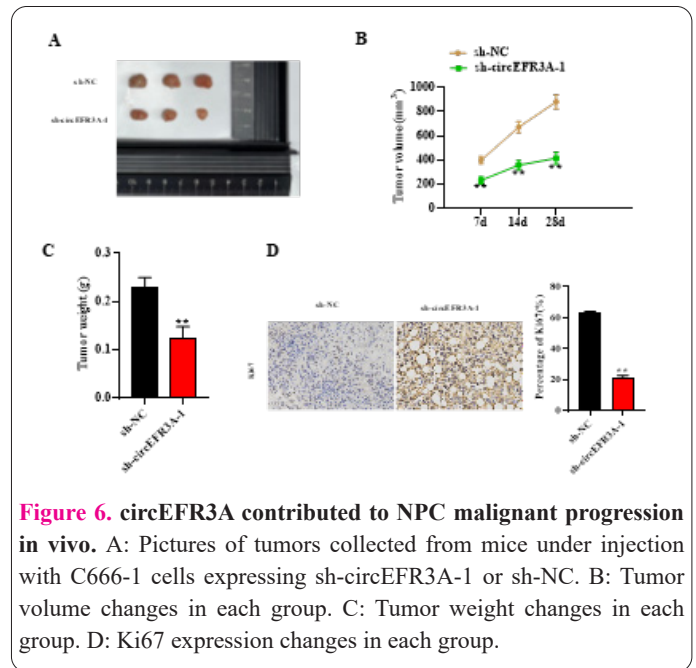
gene GOT1 (25). Consistent with the above references, our study found that circEFR3A positively modulated linear transcript EFR3A mRNA level and translation, and EFR3A presents elevation in NPC cells. circEFR3A may regulate EFR3A in NPC cells in ceRNA manner. CeRNA pattern connects the function of protein-coding mRNAs with that of non-coding RNAs such as microRNAs, long noncoding RNAs, pseudogenic RNAs and circRNAs (17). Considering that any transcripts possessing miRNA response elements can serve as ceRNAs in theory, they might represent a widespread form of post-transcriptional regulation on gene expression in both physiology and pathology (17). In addition, miRNAs exert post-transcriptional functions in cancer progression by binding to the 3'-UTR of mRNAs, leading to mRNA degradation or translational suppression (26). Herein, bioinformatics identified miR-654-3p as a common miRNA of circEFR3A and EFR3A. Previously, miR-654-3p represses cell proliferation but facilitates apoptosis via downregulating RASAL2 in non-small-cell lung cancer (27). miR-654-3p predicts poor prognosis of hepatocellular carcinoma and suppresses tumor cell growth (28). Herein, miR-654-3p showed downregulation in NPC cells, and mechanistically, miR-654-3p could bind to circEFR3A and EFR3A 3'UTR in NPC cells. Simultaneously, miR-654-3p depletion rescued the reduction of EFR3A level under circEFR3A silencing. Thus, circEFR3A competitively interacts with miR-654-3p to upregulate EFR3A in NPC cells. Rescue assays demonstrated that circEFR3A facilitated NPC cell malignant phenotype via EFR3A upregulation, further supporting ceRNA pattern of circEFR3A-miR-654-3p-EFR3A in NPC cell malignancy.

There are several limitations in our study. First, the samples of our study were relatively small. In addition, whether circEFR3A promoted NPC progression via interacting with some certain signaling pathway was unknown. Therefore, more relevant experiments should be performed in the future.

Conclusion

In conclusion, circEFR3A presents upregulation and functions as an oncogene in NPC progression. circEFR3A facilitates NPC proliferation and migration through sponging miR-654-3p and upregulating EFR3A, providing a potential new direction for seeking therapeutic plans for NPC.

Data availability
Data generated in this study are available from the corresponding author under reasonable requests.

Conflict of interest
All authors confirm that there are no conflicts of interest in this study.

References

1. Bray F, Ferlay J, Soerjomataram I, Siegel RL, Torre LA, Jemal A. Global cancer statistics 2018: GLOBOCAN estimates of incidence and mortality worldwide for 36 cancers in 185 countries. CA Cancer J Clin 2018;68(6):394-424. doi: 10.3322/caac.21492.

2. Sharma U, Barwal TS, Malhotra A, Pant N, Vivek, Dey D, et al. Long non-coding RNA TINCR as potential biomarker and therapeutic target for cancer. Life Sci 2020;257:118035. doi: 10.1016/j.lfs.2020.118035.

3. Liu YP, Wen YH, Tang J, Wei Y, You R, Zhu XL, et al. Endoscopic surgery compared with intensity-modulated radiotherapy in resectable locally recurrent nasopharyngeal carcinoma: a multicentre, open-label, randomised, controlled, phase 3 trial. The Lancet Oncology 2021;22(3):381-90. doi: 10.1016/s1470-2045(20)30673-2.

4. Bolha L, Ravnik-Glavač M, Glavač D. Circular RNAs: Biogenesis, Function, and a Role as Possible Cancer Biomarkers. International journal of genomics 2017;2017:6218353. doi: 10.1155/2017/6218353.

5. Ivanov A, Memczak S, Wyler E, Torti F, Porath HT, Orejuela MR, et al. Analysis of intron sequences reveals hallmarks of circular RNA biogenesis in animals. Cell reports 2015;10(2):170-7. doi: 10.1016/j.celrep.2014.12.019.

6. Wang Y, Mo Y, Gong Z, Yang X, Yang M, Zhang S, et al. Circular RNAs in human cancer. Molecular cancer 2017;16(1):25. doi: 10.1186/s12943-017-0598-7.

7. Yang J, Gong Y, Jiang Q, Liu L, Li S, Zhou Q, et al. Circular RNA Expression Profiles in Nasopharyngeal Carcinoma by Sequence Analysis. Frontiers in oncology 2020;10:601. doi: 10.3389/fonc.2020.00601.

8. Yang G, Zhang Y, Yang J. Identification of Potentially Functional CircRNA-miRNA-mRNA Regulatory Network in Gastric Carcinoma using Bioinformatics Analysis. Medical science monitor : international medical journal of experimental and clinical research 2019;25:8777-96. doi: 10.12659/msm.916902.

9. Xiong DD, Dang YW, Lin P, Wen DY, He RQ, Luo DZ, et al. A circRNA-miRNA-mRNA network identification for exploring underlying pathogenesis and therapy strategy of hepatocellular carcinoma. Journal of translational medicine 2018;16(1):220. doi: 10.1186/s12967-018-1593-5.

10. Bai S, Wu Y, Yan Y, Shao S, Zhang J, Liu J, et al. Construct a circRNA/miRNA/mRNA regulatory network to explore potential pathogenesis and therapy options of clear cell renal cell carcinoma. Sci Rep 2020;10(1):13659. doi: 10.1038/s41598-020-70484-2.

11. Sang Y, Chen B, Song X, Li Y, Liang Y, Han D, et al. circRNA_0025202 Regulates Tamoxifen Sensitivity and Tumor Progression via Regulating the miR-182-5p/FOXO3a Axis in Breast Cancer. Mol Ther 2019;27(9):1638-52. doi: 10.1016/j.ymthe.2019.05.011.

12. Hong X, Liu N, Liang Y, He Q, Yang X, Lei Y, et al. Circular RNA CRIM1 functions as a ceRNA to promote nasopharyngeal carcinoma metastasis and docetaxel chemoresistance through upregulating FOXQ1. Mol Cancer 2020;19(1):33. doi: 10.1186/s12943-020-01149-x.

13. Hill M, Tran N. miRNA interplay: mechanisms and consequences in cancer. Dis Model Mech 2021;14(4). doi: 10.1242/dmm.047662.

14. Zhu Q, Zhang Q, Gu M, Zhang K, Xia T, Zhang S, et al. MIR106A-5p upregulation suppresses autophagy and accelerates malignant phenotype in nasopharyngeal carcinoma. Autophagy 2021;17(7):1667-83. doi: 10.1080/15548627.2020.1781368.

15. Wang J, Zhao X, Wang Y, Ren F, Sun D, Yan Y, et al. circRNA-002178 act as a ceRNA to promote PDL1/PD1 expression in lung adenocarcinoma. Cell death & disease 2020;11(1):32. doi: 10.1038/s41419-020-2230-9.

16. Zhang L, Tao H, Li J, Zhang E, Liang H, Zhang B. Comprehensive analysis of the competing endogenous circRNA-lncRNA-miRNA-mRNA network and identification of a novel potential biomarker for hepatocellular carcinoma. Aging 2021;13(12):15990-

6008. doi: 10.18632/aging.203056.

17. Qi X, Zhang DH, Wu N, Xiao JH, Wang X, Ma W. ceRNA in cancer: possible functions and clinical implications. Journal of medical genetics 2015;52(10):710-8. doi: 10.1136/jmedgenet-2015-103334.

18. Mo Y, Wang Y, Zhang S, Xiong F, Yan Q, Jiang X, et al. Circular RNA circRNF13 inhibits proliferation and metastasis of nasopharyngeal carcinoma via SUMO2. Mol Cancer 2021;20(1):112. doi: 10.1186/s12943-021-01409-4.

19. Fang X, Huang W, Wu P, Zeng J, Li X. CircRNA circTRAF3 promotes nasopharyngeal carcinoma metastasis through targeting miR-203a-3p/AKT3 axis. Pathol Res Pract 2021;221:153438. doi: 10.1016/j.prp.2021.153438.

20. Hansen TB, Jensen TI, Clausen BH, Bramsen JB, Finsen B, Damgaard CK, et al. Natural RNA circles function as efficient microRNA sponges. Nature 2013;495(7441):384-8. doi: 10.1038/nature11993.

21. Yang N, Wang H, Zhang L, Lv J, Niu Z, Liu J, et al. Long non-coding RNA SNHG14 aggravates LPS-induced acute kidney injury through regulating miR-495-3p/HIPK1. Acta Biochim Biophys Sin (Shanghai) 2021;53(6):719-28. doi: 10.1093/abbs/gmab034.

22. Zhou D, Yang L, Zheng L, Ge W, Li D, Zhang Y, et al. Exome capture sequencing of adenoma reveals genetic alterations in multiple cellular pathways at the early stage of colorectal tumorigenesis. PloS one 2013;8(1):e53310. doi: 10.1371/journal.pone.0053310.

23. Adhikari H, Kattan WE, Kumar S, Zhou P, Hancock JF, Counter CM. Oncogenic KRAS is dependent upon an EFR3A-PI4KA signaling axis for potent tumorigenic activity. Nature communications 2021;12(1):5248. doi: 10.1038/s41467-021-25523-5.

24. Li X, Wang J, Zhang C, Lin C, Zhang J, Zhang W, et al. Circular RNA circITGA7 inhibits colorectal cancer growth and metastasis by modulating the Ras pathway and upregulating transcription of its host gene ITGA7. J Pathol 2018;246(2):166-79. doi: 10.1002/path.5125.

25. Zhou S, Guo Z, Lv X, Zhang X. CircGOT1 promotes cell proliferation, mobility, and glycolysis-mediated cisplatin resistance via inhibiting its host gene GOT1 in esophageal squamous cell cancer. Cell Cycle 2022;21(3):247-60. doi: 10.1080/15384101.2021.2015671.

26. Fabian MR, Sonenberg N, Filipowicz W. Regulation of mRNA translation and stability by microRNAs. Annu Rev Biochem 2010;79:351-79. doi: 10.1146/annurev-biochem-060308-103103.

27. Xiong J, Xing S, Dong Z, Niu L, Xu Q, Li Y, et al. miR-654-3p suppresses cell viability and promotes apoptosis by targeting RASAL2 in non-small-cell lung cancer. Molecular medicine reports 2021;23(2). doi: 10.3892/mmr.2020.11763.

28. Yang J, Zhang Z, Chen S, Dou W, Xie R, Gao J. miR-654-3p predicts the prognosis of hepatocellular carcinoma and inhibits the proliferation, migration, and invasion of cancer cells. Cancer biomarkers : section A of Disease markers 2020;28(1):73-9. doi: 10.3233/cbm-191084.